Electronic Supplementary Material (ESI) for Journal of Materials Chemistry C.

Supplementary Materials

A ferromagnetic composite of PEDOT:PSS and nitrogen-graphene decorated with copper oxide nanoparticles with high anisotropic thermoelectric properties

Ahmed Gamal El-Shamy *

Physics Department, Faculty of Science, Suez Canal University, Ismailia, Egypt

*Corresponding author; Ahmed .G. El-Shamy
E-mail: Ahmed_Khalil@science.suez.edu.eg; agabedelazim@yahoo.com

*Corresponding author; Ahmed .G. El-Shamy E-mail: Ahmed_Khalil@science.suez.edu.eg; agabedelazim@yahoo.com

S1 Materials and measurements

The conductivity measurement was performed as; the films were cut into rectangular shape (strips) and then coated with silver paste in both sides (sandwich like) in order to measure the vertical electrical conductivity of the films as in (Fig S1a) by using (Keithley 6517B) electrometer. The Equation σ = d/RA (Scm^{-1}) was applied to determine the conductivity, where (A) is the area of electrodes, (d) is the thickness of the film and R is the resistance of the film. The parallel conductivity was measured by the four probe method (Fig S1b)

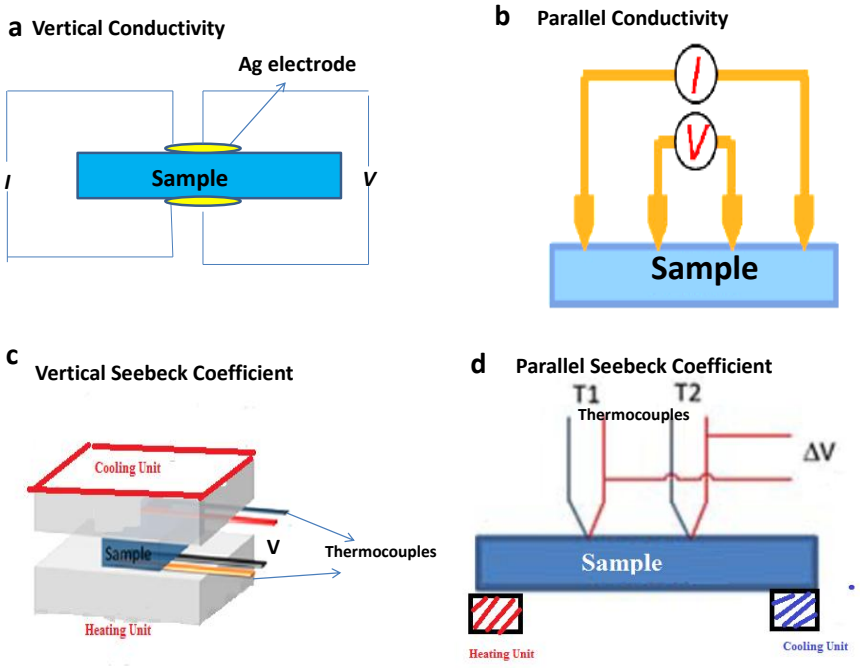

Fig S1 offers (a) the vertical and (b) parallel electrical conductivity measurements of the systems. (c) The vertical Seebeck Coefficient measurements (d) the parallel Seebeck Coefficient measurements

The films were cut into strips and coated with Ag paste, then placed between two Peltier units (heating and cooling units) in order to measure the vertical $S_{\perp}$ values of films (Fig S1c). The parallel $S_{//}$ values were measured by four probe method (Fig S1d). Nanovoltmeter (Keithley 616) was applied to detect the output voltage, which is thermally generated between the two ends of the strip that are connected with Cu wires.

S2. The Size distribution map of CuO

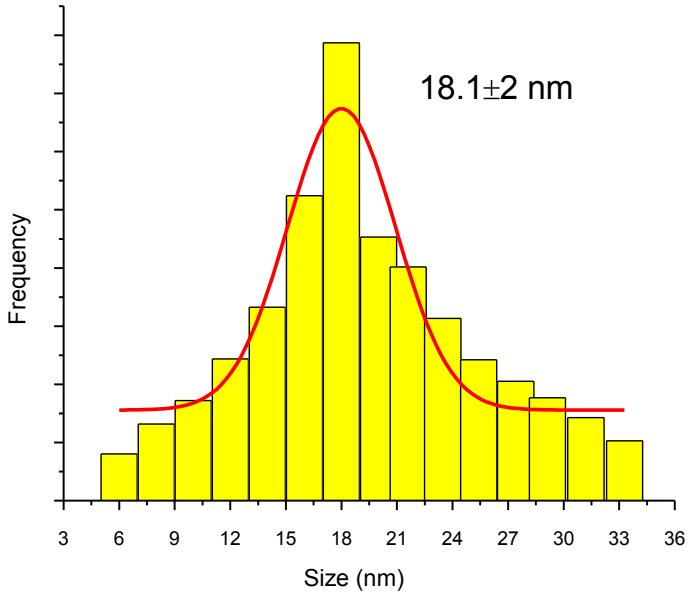

Fig S2 the size distribution map of CuO nanoparticles

S3. Magnetic behavior of CuO

Actually, the bulk copper oxide is an anti-ferromagnetic material. The anti-ferromagnetic orders are produced from the complete spin compensation due to the super-exchanges (interactions) between the (Cu^{2+}) cations and the (O^{2-}) anions.[1] This indicates that the magnetic moment per particle is zero. The hysteresis loops were performed to detect the magnetization (M_s). As discovered, the CuO has a small hysteresis area, indicating a weak ferromagnetic order. This is due to the destruction of many atomic bonds on CuO surface in the nano-scale particle produces uncompensated magnetic moment.[2] Besides, the intrinsic defects (oxygen vacancies) in the semiconducting oxides can create magnetic order.[3] Many works in the literature have detected the ferromagnetic feature of CuO nanoparticles before the Néel transition temperature of the bulk ones.[1–3]

Furthermore, the ferromagnetic properties of many oxides and metals with non-magnetic character (such as ZnO, SnO_2, Al_2O_3, CdSe, In_2O_3, and CeO_2) have been noticed at R.T when their sizes are reduced to the nano-domain.[4] The improvement in the ferromagnetic order by reducing the size was detected for several CuO nanostructures prepared with chemical approaches.[5] As

seen, no saturation is detected up to a magnetic field of about 4000 Oe due to the nano-scale dimension of CuO.[5] As detected, CuO nanoparticle has an *Ms* ~ 4.8×10^{-1} emu g^{-1}. The ferromagnetic CuO nanoparticle can display a spin-Seebeck coefficient (SSC) which has a great advantage in improving the *S* of the produced film.

S4. The statistical distance between CuO nanoparticles

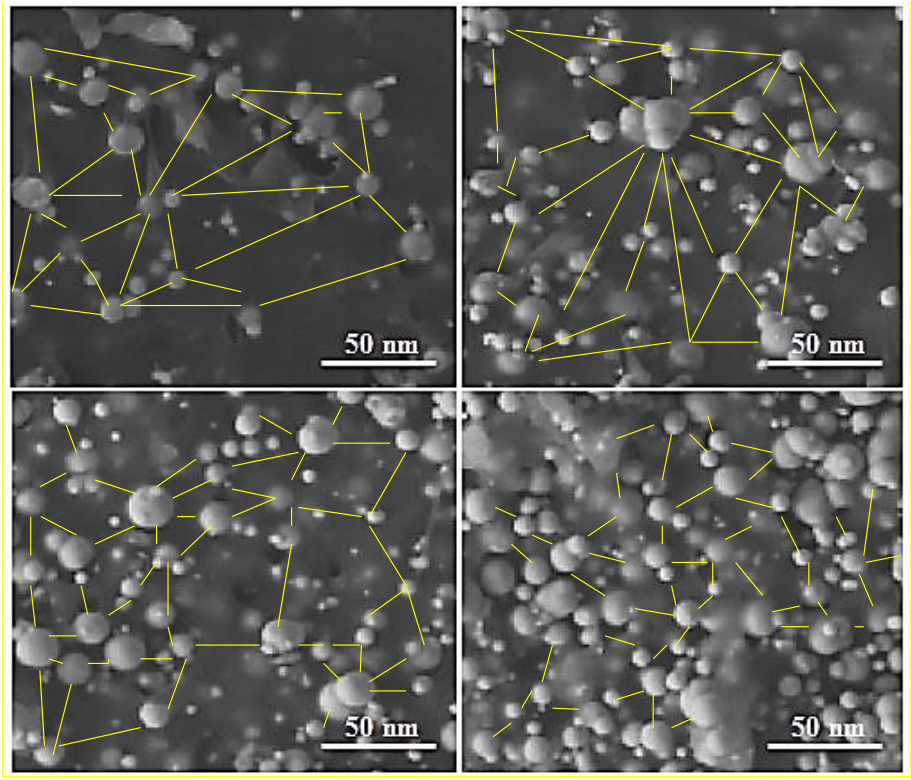

Fig. S4 The scanning electron microscope micrographs of the films for different CuO content with scale bar 50 nm.

S5 The surface SEM micrographs of the PP/^{CuO}NG films

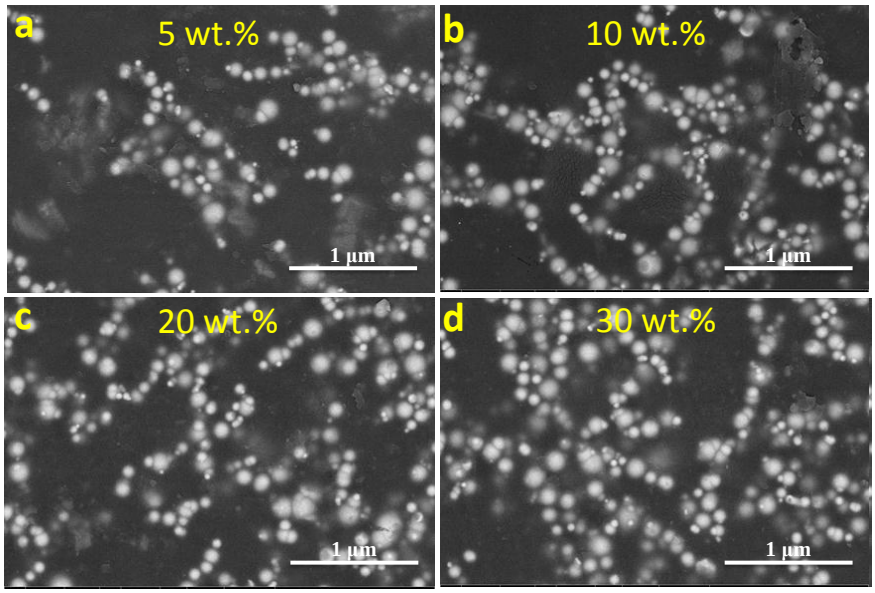

Fig. S5 The surface scanning electron microscope micrographs of the PP/^{CuO}NG films (a) 5 wt.% (b) 10 wt.% (c) 20 wt.% and (d) 30 wt.%.

Fig. S5 presents the surface-SEM scan of the PP/^{CuO}NG systems. For PP/^{CuO}NG (5 wt.% CuO) system, there are some CuO particles appeared on the system surface, however the NG sheets don't not appear, indicating the excellent embedding of NG sheets into the PP matrix (Fig S5a). For PP/^{CuO}NG (10 and 20 wt.% CuO) system, the number of CuO nanoparticles increases on the system surface with a good ^{CuO}NG dispersion, an even distribution and high compatibility in the PP template (Fig. S5b and c). On the other hand, for the PP/^{CuO}NG (30 wt.% CuO) film, great numbers of CuO nanoparticles (a huge density) appeared on the system surface with a good distribution and more compatibility with the PP template (Fig S5d). It is important to mention that (i) the (inter-) distance (space) between the CuO particles decreases with the increase in CuO addition. (ii) The high compatibility of NG in the template due to its π-π interaction with PP chains.

S6. The thickness of the film

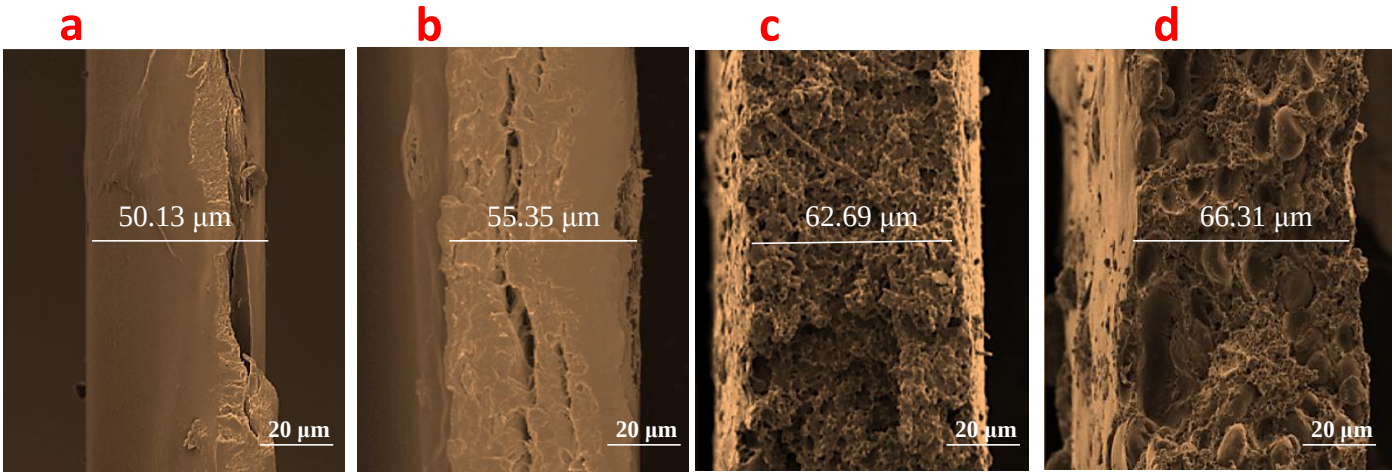

Fig S6 The cross sectional SEM micrographs of the PP/^{CuO}NG films with various CuO content (a) 5 wt.%, (b) 10 wt. %, (c) 20 wt.%, (d) 30 wt.%, displaying the well- distribution and good dispersion of CuO in the films.

S7. The anisotropic electrical conductivity and anisotropic Seebeck coefficient of PP/GR films

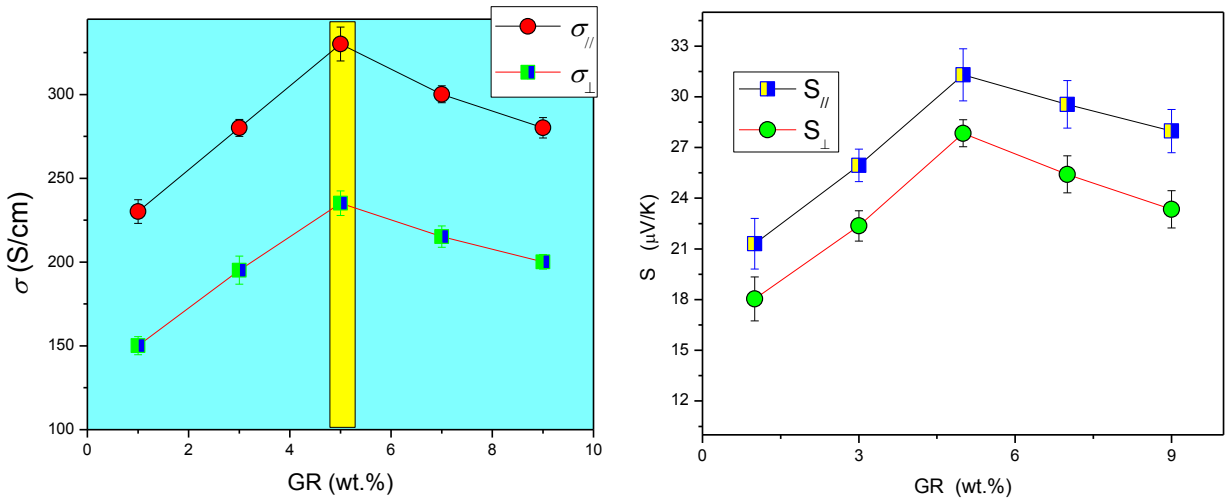

Fig S7 The anisotropic electrical conductivity and anisotropic Seebeck coefficient of PP/GR films with various GR content

S8. Raman spectra of PP/^{CuO}NG films

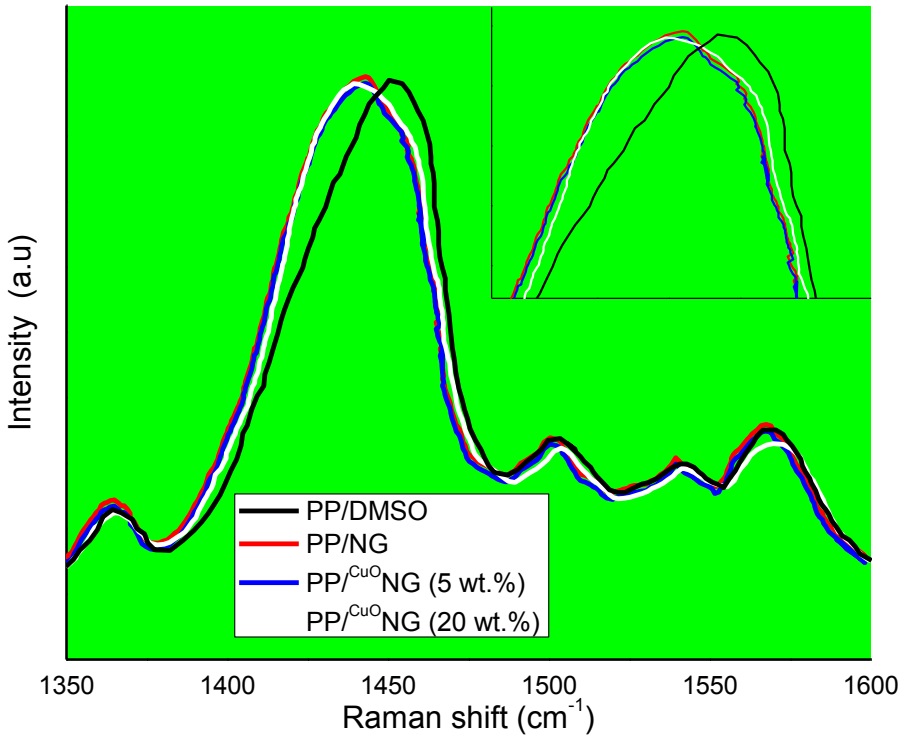

Fig S8 Raman spectra of PP/^{CuO}NG films

Raman studies of the PP/DMSO, PP/NG, and PP/^{CuO}NG (5 wt.%) and PP/^{CuO}NG (20 wt.%) films are presented in Fig S8. For PP/DMSO, two chief patterns were observed at 1366 cm^{-1} and 1451.9 cm^{-1} for the stretching vibrational modes of the single C–C bond and symmetrical C_α=C_β for PEDOT thiophene rings.[6] Significantly, a red shift in the C_α=C_β position to the lower wavenumber (shifted to 1442.5 cm^{-1}) was observed for PP/NG system relative to the PP/DMSO. This shift denotes the change in resonant structure from benzoid to quinoid structures.[7,8] However, after embedding the 5 wt.% CuO into the matrix, there is a very slightly effect on the conformation arrangement of PEDOT. However, for 20 wt.% CuO addition, a red shift in the C_α=C_β position to a lower wavenumber (higher wavelength) was also observed, proving the existence of a greater number of quinoid structures than the benzoid structures as a result of the CuO addition, which helps in improving the planarity, providing more effective delocalization charges, increasing the packing orders,[9] reduceing the carrier hopping barriers, increasing μ and hence σ.

References

1 D. Liu, D. Li, D. Yang, *AIP Advances* **2017**, 7, 015028
2 B. G. Ganga, Manoj Raama Varma, P.N. Santhosh, *Eng. Comm*. **2015**, 17, 7086–7093.
3 D. Vikraman, H. J. Park, S. –I. Kim, M. Thaiyan, *J. Alloy Comp.* **2016**, 686, 616–627
4 S. Tiwari, K. Rajeev, *Phys. Rev. B* **2005**, 72, 104433
5 E. M. M. Ibrahim, *J. Appl. Phys.* **2013**, 113, 154301
6 D. Yoo, J. Kim, S.H. Lee, W. Cho, H.H. Choi, F.S. Kim, J.H. Kim, J. Mater. Chem. A **2015**, 3, 6526–6533
7 J. Ouyang, Q. Xu, C.-W. Chu, Y. Yang, G. Li, J. Shinar, Polymer **2004,** 45, 8443-8450.
8 C.C. Yang, S. Li, J. Phys. Chem. B **2008**, 112, 14193e14197
9 A. G. El-Shamy, Mater Chem Phys **2021**, 257, 123762